

Thermoplastic PLA-LCP Composites: A Route toward Sustainable, Reprocessable, and Recyclable Reinforced Materials

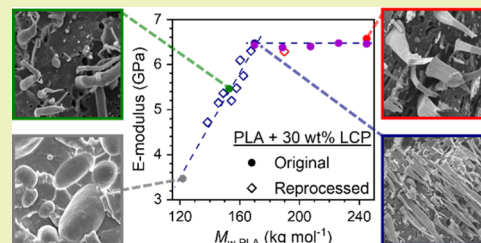
Gijs W. de Kort,* Lucienne H.C. Bouvrie, Sanjay Rastogi,[†] and Carolus H. R. M. Wilsens*[‡]

Aachen-Maastricht Institute for Biobased Materials (AMIBM), Faculty of Science and Engineering, Maastricht University, Urmonderbaan 22, 6167 RD Geleen, The Netherlands

Supporting Information

ABSTRACT: Reprocessing of reinforced composites is generally accompanied by loss of value and performance, as normally the reinforcing phase is damaged, or the matrix is lost in the process. In the search for more sustainable recyclable composite materials, we identify blends based on poly(L-lactide) (PLA) and thermotropic liquid crystalline polymers (LCP) as highly promising self-reinforced thermoplastic composites that can be recycled several times without loss in mechanical properties. For example, irrespective of the thermal history of the blend, injection molded bars of PLA containing 30 wt % LCP exhibit a tensile modulus of 6.4 GPa and tensile strength around 110 MPa, as long as the PLA matrix has a molecular weight of 170 kg mol⁻¹ or higher. However, after several mechanical reprocessing steps, with the gradual decrease in the molecular weight of the PLA matrix, deterioration of the mechanical performance is observed. The origin of this behavior is found in the increasing LCP to PLA viscosity ratio: at a viscosity ratio below unity, the dispersed LCP droplets are effectively deformed into the desired fibrillar morphology during injection molding. However, deformation of LCP droplets becomes increasingly challenging when the viscosity ratio exceeds unity (i.e., when the PLA matrix viscosity decreases during consecutive reprocessing), eventually resulting in a nodular morphology, a poor molecular orientation of the LCP phase, and deterioration of the mechanical performance. This molecular weight dependency effectively places a limit on the maximum number of mechanical reprocessing steps before chemical upgrading of the PLA phase is required. Therefore, a feasible route to maintain or enhance the mechanical properties of the blend, independent of the number of reprocessing cycles, is proposed.

KEYWORDS: mechanical reprocessing, thermotropic polyester, blend, morphology



INTRODUCTION

Plastics are an omnipresent class of materials in our current society, useful in numerous applications, though their end-of-life options require improvement: it is unacceptable for nonbiodegradable plastic waste to accumulate in our environment, neither is it desirable for plastic to accumulate in landfill. Instead, mechanical recycling, chemical recycling, or energy recovery of plastics are more preferable and sustainable solutions;^{1–5} the most preferred route is material specific and dependent on the degree of contamination^{6–8} and degradation.^{9–11} Nevertheless, it is desirable that the chosen solution provides a closed-loop, thereby minimizing both the lost value and generated waste. Generally, routes toward circularity approach the issue from a chemical point of view.¹² However, there is also significant untapped potential in mechanical recycling of materials, given that all relevant physical parameters are well understood. For example, as we will demonstrate in this work, mechanical recycling of thermoplastic composites without loss of mechanical performance can be achieved by proper identification of relevant parameters (i.e., viscosity ratio) and boundary conditions (i.e., molecular weight limitations).

Compared to the recycling of thermoplastic polymers, recycling of reinforced composites poses an additional

challenge: the composite properties are strongly dependent on the reinforcing phase. During mechanical recycling, the reinforcing phase, often brittle glass- or carbon fibers, is damaged and broken up, causing a decrease in the mechanical performance.^{13–15} Solvolysis processes have been developed that can reclaim the reinforcing fibers; however, these involve large quantities of solvents and lead to loss of the matrix phase.^{16,17} In contrast, because the mechanical performance of the composites is determined by the morphology formed during melt processing, thermoplastic composites are promising alternatives to fiber-reinforced composites, providing mechanical reinforcement while allowing for mechanical recycling at their end-of-life. To evaluate this potential, in this study we focus on the mechanical reprocessing of thermoplastic reinforced composites consisting of poly(L-lactide) (PLA) as the matrix and an aromatic thermotropic main-chain liquid crystalline polymer (LCP) as the reinforcing filler.

Thermotropic LCPs are a suitable reinforcing phase for such composites, as they are known to orient on a molecular level

Received: October 22, 2019

Revised: November 22, 2019

Published: December 10, 2019

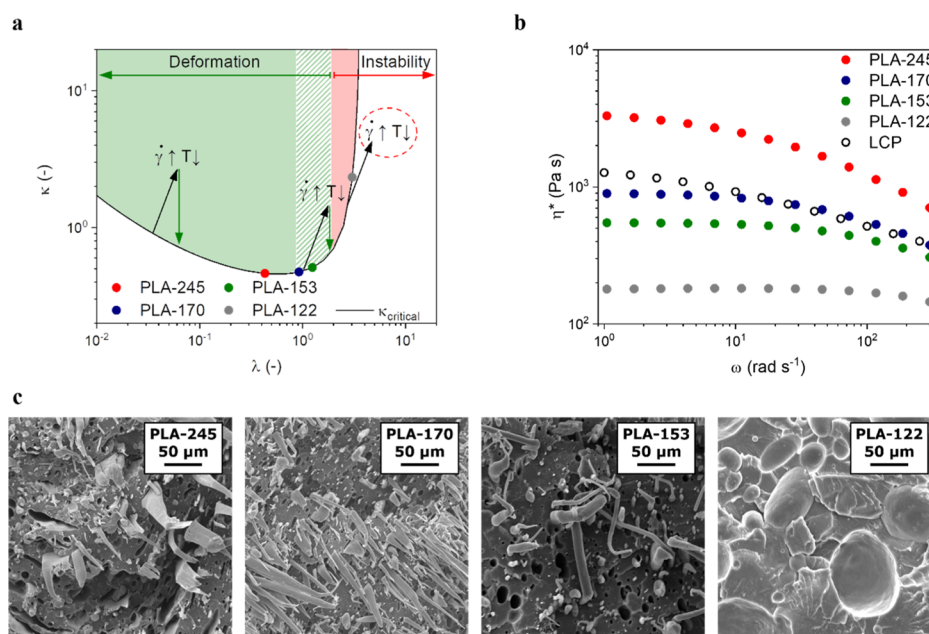


Figure 1. (a) Capillary number as a function of viscosity ratio for a shear flow field. The general effect of injection molding on the capillary number and viscosity ratio is illustrated by the arrows and different regimes with respect to the deformability of the LCP droplets are marked. Note that the points marking the observed viscosity ratios for the different PLA's shift from the region where LCP drops are easily deformed into the instable region as the M_w of the PLA decreases. (b) Viscosities of blend components measured via rheometry at 190 °C. (c) Observed morphology of composites containing 30 wt % LCP with different matrix M_w .

during flow, effectively enhancing their mechanical performance.^{18,19} This class of materials was intensively studied during the later decades of the last century and has, due to its unique properties, received renewed interest due to its potential in 3D-printing,²⁰ as strong bio-resorbable materials,²¹ and in sustainable composites.²² When dispersed in a thermoplastic matrix and upon the application of flow, LCPs can form elongated fibrils, effectively generating reinforced composites.^{23,24} The dispersion and morphology of LCP particles and chain orientation are key parameters for the performance of LCP-reinforced composites. Accordingly, the thermal and flow behavior of both phases and the processing conditions should be taken into account as these parameters determine the morphology of the dispersed LCP phase.²⁵

The high processing temperature of most commercial LCP's (generally over 300 °C) can be a limiting factor, as most thermoplastic matrices have limited stability in this temperature range. For example, PLA, as a polyester, is susceptible to degradation during processing, being sensitive to both hydrolysis and thermal degradation at elevated temperatures, resulting in a decrease in molecular weight.^{26,27} Therefore, a commercially available, amorphous LCP is used, which can be processed at temperatures as low as 220 °C.

METHODS AND MATERIALS

Materials. The PLA grades used in this study were purchased from Total Corbion [Purapol LX175 ($M_w = 245 \text{ kg mol}^{-1}$, D-content = 4%), Luminy L130 ($M_w = 170 \text{ kg mol}^{-1}$, D-content < 1%)], and Purapol L105 ($M_w = 153 \text{ kg mol}^{-1}$, D-content < 1%), abbreviated from here onwards as PLA-245, PLA-170, and PLA-153 respectively. Additionally, the Synterra PLLA 1010 grade produced by Synbra ($M_w = 122 \text{ kg mol}^{-1}$, D-content < 1%) is used and abbreviated as PLA-122. The thermotropic polyester used in this study was purchased from Celanese (Vectra LCP V400P, recommended processing temperature 200–235 °C as is also evident from the thermal behavior provided in

the Supporting Information) and is abbreviated from here onward to LCP.

Preparation and Processing of PLA–LCP Blends. The as-obtained pellets (abbreviated as sample “V” for later analysis) were dried overnight at 60 °C in vacuo prior to use. Mixtures of the respective PLA and LCP pellets were prepared in the following compositions: 0 wt % LCP (pure PLA), 10 wt % LCP, and 30 wt % LCP. The granulate mixtures were processed in the molten state using a Collin ZK 25T Teach Line twin-screw extruder at a temperature of 220 °C and a screw speed of 100 rpm and subsequently chopped into pellets. These one-time extruded pallets are abbreviated as sample “E” for later analysis.

The produced blends were molded into dog bones (2 mm × 4 mm × 80 mm, with a gauge length of 30 mm) via injection molding. A BOY XS twin-screw injection molder was used. The melt- and mold temperatures were set to 220 and 45 °C, respectively, with an injection pressure of 100 bar. After analysis, the dog bones were dried in vacuo (60 °C, overnight) and ground prior to reprocessing. The injection molded samples are abbreviated based on the number of reprocessing steps; for example, the material that was injection molded for the first time is named “R₀”, whereas the dog bones that were recycled 7 times are named “R₇”. The 30 wt % LCP composites based on PLA-245, PLA-170, PLA-153, PLA-122, and blends of PLA-245 and PLA-170 (in ratios of 100:0, 75:25, 50:50, 25:75, and 0:100) were produced via the same procedure. The PLA–LCP composite based on PLA-245 with extended extrusion time (PLA-245-E15) was extruded for 15 min in a DSM Xplore twin-screw microextruder (220 °C, 100 rpm) with a recycle prior to injection molding.

Material Characterization. The viscoelastic behavior of the pure materials was determined in a MCR 702 TwinDrive rheometer (Anton Paar) with a parallel plate geometry (diameter of 12 mm, gap of 0.7 mm). Samples were loaded at a temperature of 190 °C, and frequency sweeps were carried out with a strain of 1%. Note, rheology experiments were performed at 190 °C instead of the processing temperature of 220 °C to minimize potential thermal degradation of the recycled grades during analysis.

The mechanical properties of the composites were assessed via tensile testing, performed on a Zwick Z100. Samples were subjected to a constant deformation rate of 5 mm/min, at room temperature.

The molecular weight distributions of the PLA were obtained via gel permeation chromatography (GPC). A Shimadzu LC-2030 system was used with chloroform as the solvent, and the obtained values are relative to a polystyrene standard. Prior to injection, all samples were passed through a PTFE membrane filter with a pore size of 0.2 μm . The PLA molecular weight distribution could be determined in the case of PLA–LCP composites, as the LCP was found to be insoluble in chloroform and was eliminated from the sample upon filtration.

The microstructure of the composites was assessed via a combination of scanning electron microscopy (SEM) and polarized optical microscopy (POM). A Philips X30 microscope was used for the SEM-imaging of the fracture surfaces, at an acceleration voltage of 15 kV and magnifications of 150 \times and 1000 \times . The fracture surfaces were created by breaking samples cooled in liquid nitrogen, which were subsequently mounted and plasma-coated with a thin layer of gold. An Olympus BX53 Microscope (20 \times magnification) equipped with an Olympus DP26 camera was used for optical microscopy. To display the LCP particle morphology, the PLA phase was dissolved in chloroform, a nonsolvent for the LCP.

RESULTS AND DISCUSSION

The performance of an LCP-reinforced thermoplastic composite is mainly determined by the morphology; a fibrillar reinforcing phase with a high aspect ratio is desired (1) to achieve a high molecular orientation required for high tensile modulus and strength of the dispersed LCP phase and (2) to effectively transfer stresses from matrix to filler and prevent preliminary failure.^{23,28–31} In this study, we use commercially available polymers, being thermotropic polyester Vectra LCP V400P (LCP) and several polylactides. As explained in the Materials Section, the M_w (weight average molecular weight) of the PLA grades are 245 kg mol^{-1} (PLA-245), 170 kg mol^{-1} (PLA-170), 153 kg mol^{-1} (PLA-153), and 122 kg mol^{-1} (PLA-122). The PLA and LCP are processed together via extrusion followed by injection molding.

During the extrusion step, the LCP is dispersed in the PLA matrix through droplet breakup, facilitated by the complex combination of shear and extensional flow in the extruder.^{32,33} Deformation of droplets occurs, as the capillary number (κ , eq 1), the ratio of the hydrodynamic- and interfacial forces, exceeds unity. In the case the capillary number is larger than a critical value (κ_{critical} , Figure 1a), which depends on the flow type and viscosity ratio (λ , eq 2), the droplet stretches until κ equals the critical value and breaks up into smaller droplets as a result of the decreasing diameter. Given a sufficient amount of extrusion time, an equilibrium particle distribution is obtained as the LCP particle size will decrease until particle breakup is balanced by coalescence.

After extrusion, the blend is injection molded where it is subjected to high shear and cooling rates. During this process, the capillary number and the viscosity ratio increase (as illustrated in Figure 1a) as a consequence of the imposed cooling and increase in the deformation rate. Given that LCP droplets can only stretch into fibrils when $\kappa \gg \kappa_{\text{critical}}$, the resultant morphology and aspect ratio depend on the original viscosity ratio (and consequently on the M_w of the PLA matrix). Stable stretching of droplets is achieved at $\lambda \leq 1$ (marked in solid green in Figure 1a), whereas at higher λ droplet deformation is increasingly hindered. In the high λ regime, cooling and flow do initially facilitate droplet deformation to a smaller extent (marked in striped green in Figure 1a), but as the viscosity ratio increases further the droplets can no longer be stretched (marked in red in Figure 1a). In the latter case, the LCP droplets, having a κ smaller than κ_{critical} , are rotated by shear flow, instead of stretched. To

be more precise, the timescale required for the extensional component to stretch a droplet exceeds the timescale for rotation: the moment a droplet deforms slightly it rotates to minimize the stress it experiences and subsequently relaxes back into a sphere. This does not allow the formation of fibrils, and this is the inherent meaning of the asymptote at $\lambda = 3.8$ in Figure 1a. The increasing viscosity ratio upon cooling enhances this effect further although coalescence can still occur. For more in depth information on the topics of blend morphology and droplet deformation, the authors refer to our previous work,²² work by Utracki and Shi,²⁵ and an expansive overview on the topic by Kamal.³²

$$\kappa = \frac{\eta_{\text{matrix}} \cdot \dot{\gamma} \cdot d}{\nu_{12}} \quad (1)$$

$$\lambda = \frac{\eta_{\text{LCP}}}{\eta_{\text{matrix}}} \quad (2)$$

Figure 1b displays the complex viscosity as a function of the angular frequency for the various PLA grades and the LCP. From these data, the viscosity ratio λ can be determined at any given angular frequency, and the corresponding values (at $\omega = 100 \text{ rad s}^{-1}$, assuming the Cox–Merz relation holds) are highlighted in Figure 1a, left. Based on theory (Figure 1a), one can expect that the use of a decreasing molecular weight of PLA makes it more difficult to stretch LCP particles during injection molding, in particular for the PLA-122 sample. As mentioned earlier, under these conditions, a flow field as experienced in injection molding, having a considerable shear component, will simply result in the rotation and coalescence of droplets instead of deformation into fibrils.²⁵ Indeed, this is confirmed by analyzing the fracture morphology of the injection molded blends containing LCP and the different PLA grades in SEM analysis (Figure 1c). For the blends containing PLA-245, PLA-170, and PLA-153, a predominantly fibrillar LCP morphology is observed. As expected, the LCP phase in the blend containing PLA-122 only exhibits spherical or poorly oriented LCP particles. The effect of these changes on the orientation of the LCP is shown in the Supporting Information (Figure S1). The implications of these variations in morphology on the mechanical properties are addressed in a later section.

It is well known that PLA is susceptible to degradation processes in the melt,^{34,35} which can affect the material properties after consecutive reprocessing or recycling steps. In fact, the decrease in molecular weight is accompanied by a gradual drop in melt viscosity, mechanical properties, and an acceleration in crystallization kinetics over the course of several reprocessing cycles.^{26,27} As explained in the previous section, PLA degradation and the concomitant decrease in viscosity results in an increase in λ of the PLA–LCP blends and is thereby expected to influence both composite morphology and the mechanical performance. To investigate the effect of reprocessing on the molecular weight of the PLA matrix, a series of samples have been prepared consisting of PLA-170 and either 0, 10, or 30 wt % LCP. These samples have been analyzed in the virgin state, prior to processing (labeled V), after a one-time extrusion to create the blends (labeled E), after first-time injection molding (R_0), and after reprocessing for up to 7 cycles (R_1 to R_7). The molecular weight (M_w), zero shear viscosity (η_0^*), and LCP particle morphology have been evaluated after each cycle. An overview is provided in Figure 2.

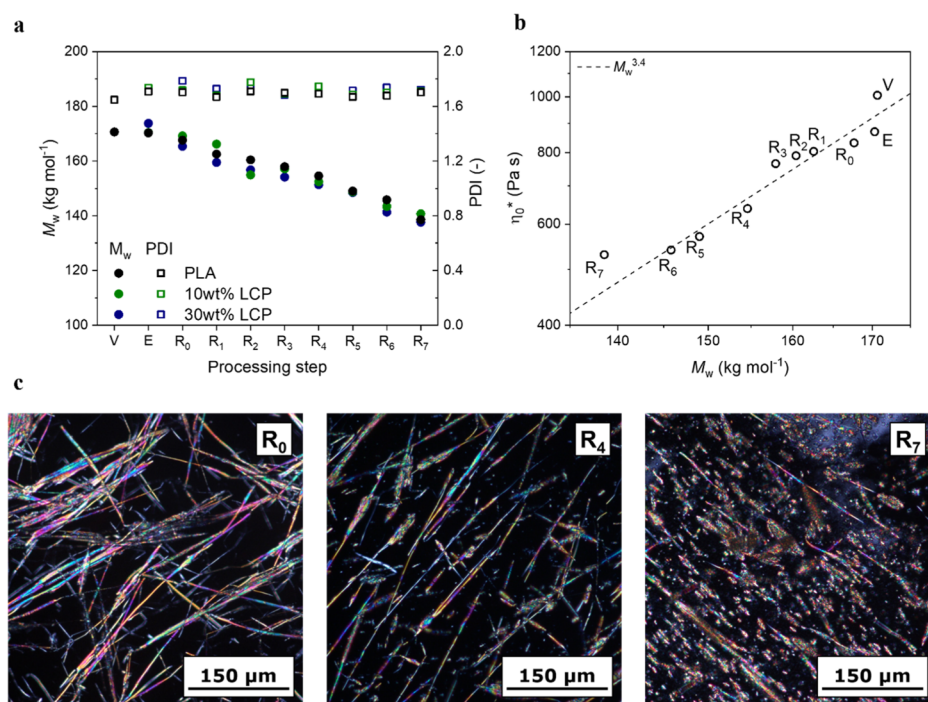


Figure 2. (a) Weight average molecular weight and polydispersity of PLA for reprocessed PLA and reprocessed composites. (b) Zero shear viscosity as function of molecular weight for reprocessed PLA-170. Frequency sweep data are available in Figure S2 of the Supporting Information. (c) Changes in LCP the particle morphology over the course of reprocessing, POM images taken under crossed-polarizers; PLA was selectively dissolved in chloroform.

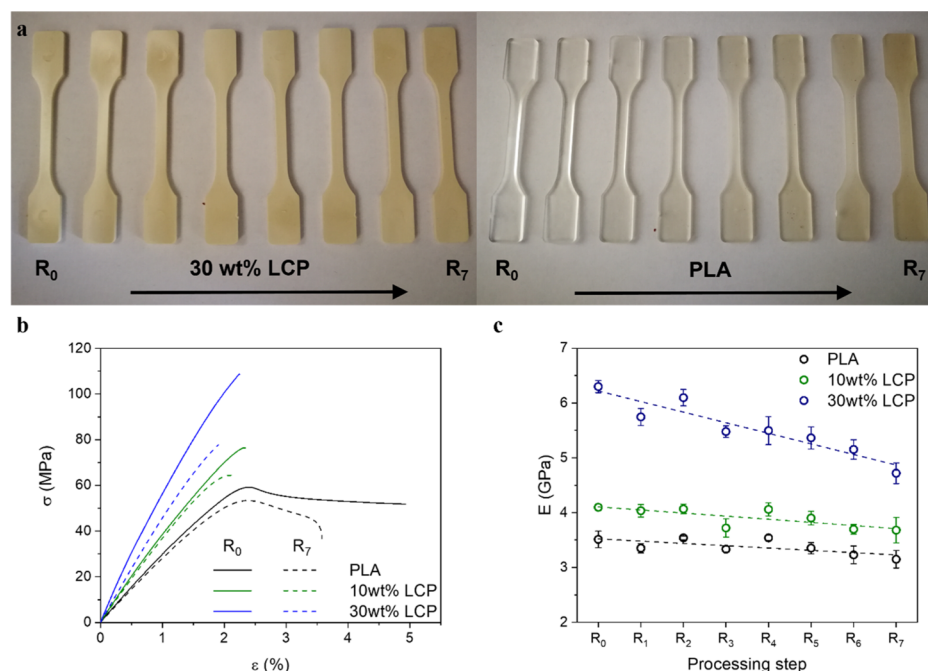


Figure 3. (a) Visual appearance of tensile bars after a specified number of reprocessing steps. (b) Characteristic stress–strain curves for the fresh materials and the materials after seven reprocessing steps. (c) Young's modulus of the reprocessed samples.

Figure 2a shows the evolution of the molecular weight (M_w) and polydispersity index of the PLA matrix, obtained from the pure PLA-170 and PLA–LCP composites after each (re)-processing cycle. As expected, we observe a gradual decrease of the molecular weight, though no change in the molecular weight distribution is observed upon consecutive reprocessing. Overall, M_w decreases by roughly 18% over the course of seven

cycles for all samples. Furthermore, it is clear that the presence of LCP as the dispersed phase does not influence the degradation process of the PLA phase during reprocessing. Corresponding to the decrease in molecular weight, the viscosity decreases with each processing or reprocessing step (Figure 2b). The zero shear viscosity (η_0^*), determined from parallel plate rheometry at 190 °C, frequency sweep data are

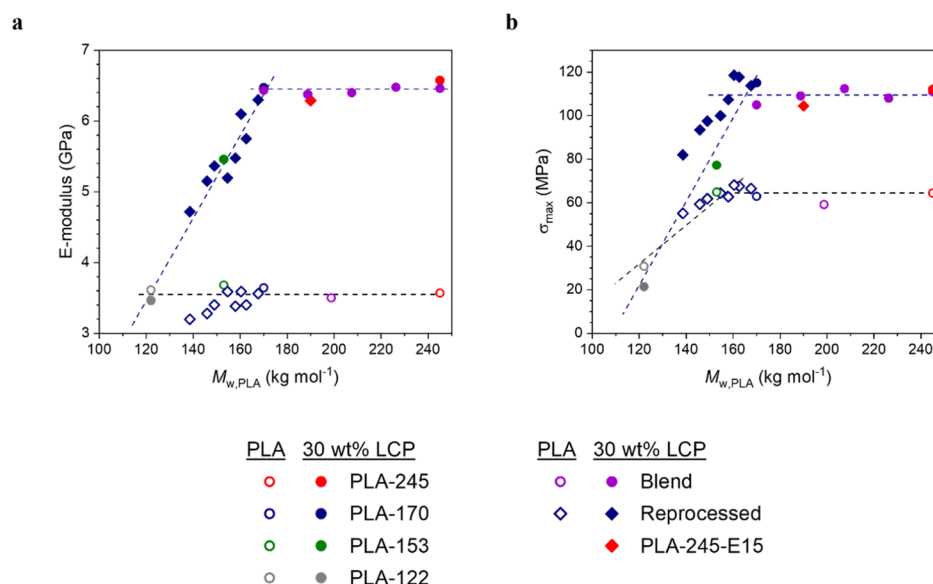


Figure 4. (a) Young's modulus of PLA and 30 wt % LCP composites as function of matrix M_w . (b) Maximum stress of PLA and 30 wt % LCP composites as function of matrix M_w . The yield stress was used as the maximum stress for the pure PLA samples, the stress at break was used as the maximum stress for the 30 wt % PLA composites.

available in Figure S2 of the [Supporting Information](#)) is shown as a function of M_w (determined by GPC), and follows the expected scaling for entangled polymer melts ($\eta_0^* \sim M_w^{3.4}$). It is noteworthy that the molecular weight and viscosity of the PLA-170 gradually decreases during consecutive reprocessing to a value somewhere between PLA-153 and PLA-122. As previously explained, this affects the obtained morphology: the gradual decrease in M_w of the PLA matrix upon reprocessing increases the viscosity ratio (λ), which limits the deformation and molecular orientation (as shown in [Figure S1](#)) of the dispersed LCP particles during injection molding. The viscoelastic response of the LCP remained unaffected by reprocessing, as shown in Figures S3 and S4 of the [Supporting Information](#). [Figure 2c](#) shows the morphology of PLA–LCP blends containing 10 wt % LCP after a different number of reprocessing cycles. The original morphology (R_0) is dominated by homogeneous fibrils with a high aspect ratio. After four reprocessing steps (R_4), the fibrils appear less homogeneous and an additional population of droplets with a low aspect ratio has appeared. Finally, after seven cycles (R_7), the morphology is dominated by slightly deformed droplets, while poorly oriented and inhomogeneous fibrils form a secondary group of particles. The LCP particle morphologies observed in POM are in line with the aforementioned theory regarding droplet behavior, as they confirm that the decrease in M_w of the PLA phase results in a gradual increase in λ and thereby alters the deformability of the LCP particles during injection molding.

An interesting difference between the reprocessed PLA and reprocessed PLA–LCP composites arises from their respective visual appearances ([Figure 3a](#)). The amorphous PLA is initially transparent, but gradually becomes hazy due to the increasing presence of crystallites and contaminants. The PLA–LCP composites, on the other hand, are opaque with a beige color and do not visually change upon reprocessing. The dispersed LCP fibrils, with particle sizes larger than the wavelengths of visible light, scatter light and thus dominate the sample appearance. This feature can be considered as beneficial from

an aesthetic perspective, at least, compared to the reprocessed PLA samples.

The mechanical performance is an important characteristic of reinforced composites and, therefore, [Figure 3b](#) displays the tensile curves of R_0 and R_7 samples with varying LCP content. In general, we observe an effective reinforcement of the PLA by the LCP phase, as the modulus and stress at break readily increase with the LCP content. However, as the PLA decreases in molecular weight and the LCP morphology changes, a clear decrease in mechanical performance is observed. This is clearly exemplified by the decrease of the Young's modulus (E) of both the PLA and the PLA–LCP blends over the course of seven reprocessing steps ([Figure 3c](#)). The modulus of the pure PLA decreases gradually upon repeated reprocessing, though the overall change is limited (<10%). In contrast, the Young's modulus of the 30 wt % LCP composites decreases with 25% after seven reprocessing steps. A similar trend was observed with respect to the maximum stress, as shown in [Figure S5](#) of the [Supporting Information](#). [Figure 4a](#) shows an overview of the Young's moduli of the injection molded dog bones of PLA and PLA–LCP blends (30 wt %) as a function of the molecular weight (M_w) of the PLA matrix. In this plot, data from composites based on (1) different virgin matrices (PLA-245 to PLA-122), (2) reprocessed PLA-170 (R_0 to R_7), (3) blends of PLA-245 and PLA-170 in different ratios, and (4) PLA-245 that was extruded for 15 min to mimic several reprocessing steps (PLA-245-E15) are combined. In the case of the pure PLA samples, the modulus remains largely unaffected by M_w , indicating that the decrease in mechanical properties upon reprocessing of pure PLA is likely correlated to the accumulation of impurities or degradation of additives. The PLA–LCP blends show an interesting trend: the Young's modulus of the blends remains constant for samples with a PLA matrix with a M_w of 170 kg mol^{-1} and higher, whereas samples with a M_w below 170 kg mol^{-1} exhibit a decreasing modulus. Whether the composites were reprocessed or not, the relation between the modulus and the M_w of the matrix remains the same. The maximum tensile stress ([Figure 4b](#)) shows the same trend with a constant value when the PLA

matrix exhibits a M_w of 170 kg mol^{-1} and higher, while decreasing when the PLA molecular weight drops below this value. This confirms that the mechanical performance of PLA–LCP composites, irrespective of the thermal history, depends mainly on the molecular weight of the PLA phase for the given processing conditions.

When comparing the relation between κ and λ (Figure 1a) and the relations between either the E -modulus or σ_{\max} as a function of $M_{w, \text{PLA}}$ (Figure 4), one can observe that these are related. With respect to the two regimes observed in the mechanical performance of the self-reinforced PLA–LCP composites, it appears that the declining $M_{w, \text{PLA}}$ upon reprocessing to values below 170 kg mol^{-1} corresponds to a value of $\lambda > 1$. Under these conditions, stable deformation of LCP particles into fibrils becomes challenging during the injection molding process.³³ The resultant morphology of a large reduction in M_w PLA is clearly evident from Figure 2c (R_7). This is not the case in the second regime ($\lambda \leq 1$, or $M_{w, \text{PLA}} \geq 170 \text{ kg mol}^{-1}$); the LCP droplets generated during extrusion can effectively deform into fibrils during injection molding, forming particles with a high aspect ratio, regardless of the precise M_w of the PLA, resulting in a constant mechanical performance. Interestingly, the process appears irrespective of the actual processing time or the degradation concomitant to prolonged processing times, as is evident for the PLA-245-E15 sample. The two regimes are morphological in origin and quite generic for composites as a similar relation is observed in fiber-reinforced composites.^{36,37}

These two regimes, in combination with the fact that the mechanical performance of the reprocessed composites matched with the other samples, have strong implications for the recycling of PLA–LCP composites and potentially thermoplastic composites in general. Our results show that PLA–LCP composites can be reprocessed without deterioration of the mechanical properties, given that the molecular weight of the PLA remains sufficiently high to allow deformation of the LCP droplets during injection molding. This reprocessability is a unique and highly desirable property in order to achieve more sustainable reinforced composites. Given that rheological behavior of the currently used LCP grade, Vectra LCP V400P, changes little under the evaluated processing conditions even after prolonged exposure to a temperature of $220 \text{ }^\circ\text{C}$, it appears that the degradation of the PLA sample is the limiting factor in the reprocessing process described above. In other words, the use of high molecular weight PLA is desired as starting material. Note that, choice of the PLA and LCP grade (with their respective molecular weights and viscosities) used to form the composite, determine the extent to which the molecular weight of the PLA is allowed to decrease until recycling without deterioration of the mechanical performance is no longer possible. Therefore, the λ of the initially produced blend is preferably around 0.1.

Overall, this bottom-up understanding for the development of reinforced thermoplastic composites that are reprocessed without loss of performance has large implication on their recyclability. However, as the molecular weight of the PLA matrix decreases with each cycle (due to both reprocessing and exposure during use), at some point the morphology of the composite, and correspondingly the performance, will deteriorate. This means that this process does not yet allow for closed-loop recycling, as the composite, or rather the PLA material eventually has to be discarded or upgraded. There are, however, well-known methods available to increase the

molecular weight of PLA, which can provide the requirements to achieve the desired closed-loop recycling process, as is illustrated in Figure 5. One approach is solid state post

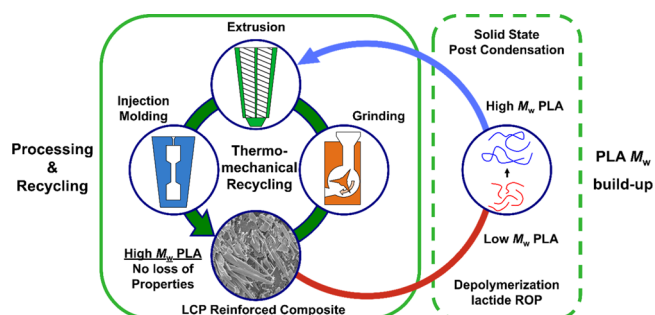


Figure 5. Overview of strategies for reprocessing (left) and enhancing the molecular weight of PLA (right). Connecting these strategies provides a route toward closed-loop recycling of LCP-reinforced composites. Extension of the work conducted on thermomechanical recycling with either SSPC or full chemical recycling of the PLA phase allows an indefinite number of use cycles without loss of mechanical properties.

condensation (SSPC), a technique widely used in polycondensates to increase the molecular weight of polymer after the initial polymerization, and it has been utilized to obtain PLA with a molecular weight well above that used in this study.³⁸ Another option is depolymerization of PLA into lactide as a product.³⁹ In turn, the reclaimed lactide can be used as feed to conduct a ring-opening polymerization, once again yielding high molecular weight PLA.⁴⁰ When required, separation of the LCP particles from the PLA phase can readily be achieved by filtration after dissolution of the PLA in common laboratory solvents such as tetrahydrofuran or chloroform, which are nonsolvents for the LCP phase. Additional resources required in these processes, such as energy and chemicals, increase the ecological footprint of the overall process. Note that the production of lactide via chemical depolymerization of PLA requires less energy and resources compared to production of lactide via the fermentation of biomass.³⁹ The increased environmental impact due to the need to maintain a minimum PLA molecular weight diminishes quickly, however, considering that the PLA produced in these processes is of a high enough molecular weight and the composites performance can be maintained over multiple thermomechanical recycling steps.

Last, it is noteworthy to highlight that the deformation, breakup, and coalescence of droplets in a matrix are mainly governed by physical parameters and are not specific to the chemical composition of the blend.³² The findings and insight reported in this study are not necessarily limited to the combination of PLA and LCP, as the theoretical framework holds for any thermoplastic blend. A similar window, where the performance can be maintained upon thermomechanical recycling, is likely to be available in other immiscible thermoplastic composites, as long as the thermal and physical behavior of both phases matches.

CONCLUSIONS

We have demonstrated the reprocessability and excellent mechanical performance of thermoplastic composites containing PLA as a matrix and a thermotropic LCP as a reinforcing phase. The mechanical performance of the composites appears

strongly dependent on the viscosity ratio between the two components as this governs the resultant LCP morphology after injection molding. However, because of thermal degradation from processing, the molecular weight of the PLA matrix is found to decrease gradually with each reprocessing cycle, resulting into a successive decrease in the LCP particle orientation and retrospectively decreasing the mechanical performance of the composite. The molecular weight of the PLA matrix is identified as the dominant parameter in this process, as data from composites with different PLA grades and varying molecular weights match excellently with recycled composites.

Two distinct regimes, dependent on the LCP/PLA viscosity ratio are identified: in the first regime ($\lambda < 1$), an increase in matrix viscosity results in a slightly coarser morphology; however, the overall mechanical performance is not effected as the LCP is still present in the form of long, thin fibrils, and the degree of LCP orientation remains high. In the second regime ($\lambda > 1$), a decrease in matrix viscosity results in less favorable LCP morphology as the matrix is less effective in deforming the molten LCP. At high viscosity ratio ($\lambda \approx 3.5$), a complete lack of droplet deformation by a shear flow field is caused: the LCP is present in the form of large nodules. Accordingly, the mechanical performance of the composite decreases as the LCP morphology changes with lower matrix molecular weight.

In the regime where the viscosity ratio of the blend is low ($\lambda < 1$), the mechanical performance of melt-processable LCP/PLA composites does not decrease upon recycling. This regime can be obtained readily from the thermal- and flow behavior of the LCP- and matrix phase. As basis for this regime stems from the flow behavior and morphology development, it is a generic feature of blends and not limited to LCP/PLA systems. These findings might prove useful in the search for recyclable and sustainable composite materials.

■ ASSOCIATED CONTENT

Supporting Information

The Supporting Information is available free of charge at <https://pubs.acs.org/doi/10.1021/acssuschemeng.9b06305>.

Additional information on WAXD diffractograms and orientation parameter as function of matrix M_w , complex viscosity of PLA-170 after each reprocessing cycle, stability of the LCP under the applied reprocessing conditions, development of the maximum tensile stress over the course of seven reprocessing cycles, and thermal behavior of LCP and PLA-170 (PDF)

■ AUTHOR INFORMATION

Corresponding Authors

*E-mail: gijs.dekort@maastrichtuniversity.nl (G.W.d.K.).

*E-mail: karel.wilsens@maastrichtuniversity.nl (C.H.R.M.).

ORCID

Sanjay Rastogi: 0000-0002-7804-7349

Carolus H. R. M. Wilsens: 0000-0003-3063-9510

Notes

The authors declare no competing financial interest.

■ ACKNOWLEDGMENTS

The research leading to these results has received funding by the H2020 Framework Program of the European Union under grant agreement no. 685614. Vectra LCP 400P grade is a

registered trademark of Celanese Corporation, Dallas, TX. The material composition, as well as the results associated with this material are the property of Celanese Corporation. NWO (Nederlandse Organisatie voor Wetenschappelijk Onderzoek) is acknowledged for providing beam time at the ESRF. The staff of the DUBBLE (Dutch Belgian beamline, ESRF) are acknowledged for supporting the X-ray experiments.

■ REFERENCES

- (1) Al-Salem, S. M.; Lettieri, P.; Baeyens, J. Recycling and Recovery Routes of Plastic Solid Waste (PSW): A Review. *Waste Manag.* **2009**, *29*, 2625–2643.
- (2) Rahimi, A.; Garca, J. M. Chemical Recycling of Waste Plastics for New Materials Production. *Nat. Rev. Chem.* **2017**, *1*. DOI: 10.1038/s41570-017-0046
- (3) Perugini, F.; Mastellone, M. L.; Arena, U. A Life Cycle Assessment of Mechanical and Feedstock Recycling Options for Management of Plastic Packaging Wastes. *Environ. Prog.* **2005**, *24*, 137–154.
- (4) Asmatulu, E.; Twomey, J.; Overcash, M. Recycling of Fiber-Reinforced Composites and Direct Structural Composite Recycling Concept. *J. Compos. Mater.* **2014**, *48*, 593–608.
- (5) Shuaib, N. A.; Mativenga, P. T. Energy Demand in Mechanical Recycling of Glass Fibre Reinforced Thermoset Plastic Composites. *J. Clean. Prod.* **2016**, *120*, 198–206.
- (6) Luijsterburg, B.; Goossens, H. Assessment of Plastic Packaging Waste: Material Origin, Methods, Properties. *Resour. Conserv. Recycl.* **2014**, *85*, 88–97.
- (7) Jansen, M.; Thoden van Velzen, U.; Pretz, T. *Handbook for Sorting of Plastic Packaging Waste Concentrates: Separation Efficiencies of Common Plastic Packaging Objects in Widely Used Separation Machines at Existing Sorting Facilities with Mixed Postconsumer Plastic Packaging Waste as Input*; Wageningen University & Research, 2015.
- (8) Luijsterburg, B. J.; Jobse, P. S.; Spoelstra, A. B.; Goossens, J. G. P. Solid-State Drawing of Post-Consumer Isotactic Poly(Propylene): Effect of Melt Filtration and Carbon Black on Structural and Mechanical Properties. *Waste Manag.* **2016**, *54*, 53–61.
- (9) Teteris, G. Degradation of Polyolefines during Various Recovery Processes. *Macromol. Symp.* **1999**, *144*, 471–479.
- (10) Jin, H.; Gonzalez-Gutierrez, J.; Oblak, P.; Zupancic, B.; Emri, I. The Effect of Extensive Mechanical Recycling on the Properties of Low Density Polyethylene. *Polym. Degrad. Stab.* **2012**, *97*, 2262–2272.
- (11) Choudhury, A.; Mukherjee, M.; Adhikari, B. Thermal Stability and Degradation of the Post-Use Reclaim Milk Pouches during Multiple Extrusion Cycles. *Thermochim. Acta* **2005**, *430*, 87–94.
- (12) Christensen, P. R.; Scheuermann, A. M.; Loeffler, K. E.; Helms, B. A. Closed-Loop Recycling of Plastics Enabled by Dynamic Covalent Diketoneamine Bonds. *Nat. Chem.* **2019**, *11*, 442–448.
- (13) Eriksson, P.-A.; Albertsson, A.-C.; Boydell, P.; Prautzsch, G.; Manson, J.-A. E. Prediction of Mechanical Properties of Recycled Fiberglass Reinforced Polyamide 66. *Polym. Compos.* **1996**, *17*, 830–839.
- (14) Kuram, E.; Tasci, E.; Altan, A. I.; Medar, M. M.; Yilmaz, F.; Ozelik, B. Investigating the Effects of Recycling Number and Injection Parameters on the Mechanical Properties of Glass-Fibre Reinforced Nylon 6 Using Taguchi Method. *Mater. Des.* **2013**, *49*, 139–150.
- (15) Le Duigou, A.; Pillin, I.; Bourmaud, A.; Davies, P.; Baley, C. Effect of Recycling on Mechanical Behaviour of Biocompostable Flax/Poly(l-Lactide) Composites. *Compos. Part A Appl. Sci. Manuf.* **2008**, *39*, 1471–1478.
- (16) Morin, C.; Loppinet-Serani, A.; Cansell, F.; Aymonier, C. Near- and Supercritical Solvolysis of Carbon Fibre Reinforced Polymers (CFRPs) for Recycling Carbon Fibers as a Valuable Resource: State of the Art. *J. Supercrit. Fluids* **2012**, *66*, 232–240.
- (17) Iwaya, T.; Tokuno, S.; Sasaki, M.; Goto, M.; Shibata, K. Recycling of Fiber Reinforced Plastics Using Depolymerization by

Solvothermal Reaction with Catalyst. *J. Mater. Sci.* **2008**, *43*, 2452–2456.

(18) Chung, T.-S. The Recent Developments of Thermotropic Liquid Crystalline Polymers. *Polym. Eng. Sci.* **1986**, *26*, 901–919.

(19) Aciermo, D.; La Mantia, F. P.; Polizzotti, G.; Ciferri, A.; Valenti, B. Ultra-high modulus liquid crystalline polyesters. p-Hydroxybenzoic acid copolyesters. *Macromolecules* **1982**, *15*, 1455–1460.

(20) Gantenbein, S.; Masania, K.; Woigk, W.; Sesseg, J. P. W.; Tervoort, T. A.; Studart, A. R. Three-Dimensional Printing of Hierarchical Liquid-Crystal-Polymer Structures. *Nature* **2018**, *561*, 226–230.

(21) Montes de Oca, H.; Wilson, J. E.; Penrose, A.; Langton, D. M.; Dagger, A. C.; Anderson, M.; Farrar, D. F.; Lovell, C. S.; Ries, M. E.; Ward, I. M.; et al. Liquid-Crystalline Aromatic-Aliphatic Copolyester Bioresorbable Polymers. *Biomaterials* **2010**, *31*, 7599–7605.

(22) de Kort, G. W.; Rastogi, S.; Wilsens, C. H. R. M. Controlling Processing, Morphology, and Mechanical Performance in Blends of Polylactide and Thermotropic Polyesters. *Macromolecules* **2019**, *52*, 6005–6017.

(23) Kiss, G. In situ composites: Blends of isotropic polymers and thermotropic liquid crystalline polymers. *Polym. Eng. Sci.* **1987**, *27*, 410–423.

(24) DeMeuse, M. T.; Kiss, G. *Liquid Crystal Polymers (LCPs) as a Reinforcement in High Temperature Polymer Blends*; Woodhead Publishing Limited, 2014.

(25) Utracki, L. A.; Shi, Z. H. Development of polymer blend morphology during compounding in a twin-screw extruder. Part I: Droplet dispersion and coalescence? a review. *Polym. Eng. Sci.* **1992**, *32*, 1824–1833.

(26) Pillin, I.; Montrelay, N.; Bourmaud, A.; Grohens, Y. Effect of Thermo-Mechanical Cycles on the Physico-Chemical Properties of Poly(Lactic Acid). *Polym. Degrad. Stab.* **2008**, *93*, 321–328.

(27) Badia, J. D.; Strömberg, E.; Karlsson, S.; Ribes-Greus, A. Material Valorisation of Amorphous Polylactide. Influence of Thermo-Mechanical Degradation on the Morphology, Segmental Dynamics, Thermal and Mechanical Performance. *Polym. Degrad. Stab.* **2012**, *97*, 670–678.

(28) Blizard, K. G.; Baird, D. G. The Morphology and Rheology of Polymer Blends Containing a Liquid Crystalline Copolyester. *Polym. Eng. Sci.* **1987**, *27*, 653–662.

(29) Blizard, K. G.; Federici, C.; Federico, O.; Chapoy, L. L.; Caduti, V. The Morphology of Extruded Blends Containing a Thermotropic Liquid Crystalline Polymer. *Polym. Eng. Sci.* **1990**, *30*, 1442–1453.

(30) Bassett, B. R.; Yee, A. F. A Method of Forming Composite Structures Using In Situ-Formed Liquid Crystal Polymer Fibers in a Thermoplastic Matrix. *Polym. Compos.* **1990**, *11*, 10–18.

(31) Silverstein, M. S.; Hiltner, A.; Baer, E. Hierarchical Structure in LCP/PET Blends. *J. Appl. Polym. Sci.* **1991**, *43*, 157–173.

(32) Kamal, M. R.; Utracki, L. A.; Mirzadeh, A. Rheology of Polymer Alloys and Blends. In *Polymer Blends Handbook*; Utracki, L. A., Wilkie, C., Eds.; Springer Netherlands: Dordrecht, 2014; Vol. 2, pp 726–853.

(33) Heino, M. T.; Hietaoja, P. T.; Vaimio, T. P.; Seppälä, J. V. Effect of Viscosity Ratio and Processing Conditions on the Morphology of Blends of Liquid Crystalline Polymer and Polypropylene. *J. Appl. Polym. Sci.* **1994**, *51*, 259–270.

(34) Auras, R. *Poly(Lactic Acid) Synthesis, Structures, Properties, Processing, and Application*; Auras, R., Lim, L., Selke, S., Tsuji, H., Eds.; John Wiley & Sons, Inc.: Hoboken, 2010.

(35) Dorgan, J. R.; Janzen, J.; Clayton, M. P.; Hait, S. B.; Knauss, D. M. Melt rheology of variable L-content poly(lactic acid). *J. Rheol.* **2005**, *49*, 607.

(36) Thomason, J. L.; Vlug, M. A. Influence of Fibre Length and Concentration on the Properties of Glass Fibre-Reinforced Polypropylene: 1. Tensile and Flexural Modulus. *Compos. Part A Appl. Sci. Manuf.* **1996**, *27*, 477–484.

(37) Thomason, J. L.; Vlug, M. A.; Schipper, G.; Krikor, H. G. L. T. Influence of Fibre Length and Concentration on the Properties of Glass Fibre-Reinforced Polypropylene: Part 3. Strength and Strain at Failure. *Compos. Part A Appl. Sci. Manuf.* **1996**, *27*, 1075–1084.

(38) Peng, B.; Hou, H.; Song, F.; Wu, L. Synthesis of High Molecular Weight Poly(l-lactic acid) via Melt/Solid State Polycondensation. II. Effect of Precrystallization on Solid State Polycondensation. *Ind. Eng. Chem. Res.* **2012**, *51*, 5190–5196.

(39) Piemonte, V.; Sabatini, S.; Gironi, F. Chemical Recycling of PLA: A Great Opportunity Towards the Sustainable Development? *J. Polym. Environ.* **2013**, *21*, 640–647.

(40) Nijenhuis, A. J.; Grijpma, D. W.; Pennings, A. J. Lewis Acid Catalyzed Polymerization of L-Lactide. Kinetics and Mechanism of the Bulk Polymerization. *Macromolecules* **1992**, *25*, 6419–6424.